Available online at www.sciencedirect.com
ScienceDirect
Journal of Sound and Vibration 306 (2007) 835–848
JOURNAL OF SOUND AND VIBRATION
www.elsevier.com/locate/jsvi

A new method for line spectra reduction similar to generalized synchronization of chaos

Xiang Yu*, Shijian Zhu, Shuyong Liu

Institute of Noise and Vibration, Naval University of Engineering, Wuhan 430033, PR China

Received 30 December 2006; received in revised form 24 May 2007; accepted 30 June 2007

Abstract

Line spectra in the radiated noise of marine vessels are the most visible signs, which can be detected, tracked and identified by enemy's passive sonar, and hence it is of great significance to reduce the line spectra for improving the acoustic stealth of marine vessels. In this paper, a driving parameter scheme using an external chaotic signal to drive a nonlinear vibration isolation system (VIS) of onboard machinery is presented to make the chaotic motion in the nonlinear VIS persistent, which is similar to generalized synchronization of chaos in some sense. In this way, the line spectra in the radiated noise can be reduced effectively because the response spectrum of a chaotic system under harmonic excitations is a continuous and reduced one. Numerical simulations are carried out and the results confirm the effectiveness of this method. The maximum conditional Lyapunov exponent is calculated numerically and its negative value indicates the stability of this driving parameter control scheme.

1. Introduction

Chaos has been extensively studied in the past decade within the scientific, engineering and mathematical fields. From traditional viewpoint, chaos is an undesirable phenomenon because of its complex and unpredictable motion. Many researchers have devoted themselves to find new ways to suppress chaos or stabilize chaotic motions into periodic behaviors more efficiently. However, recently, more and more achievements about the natural features of chaos display that chaos is desirable under certain circumstances. For example, chaos is important in secure communication, information processing, liquid mixing, biological systems, etc. [1–3].

Another potential application of chaos in engineering, namely using chaos to reduce line spectra in the radiated noise of marine vessels, was presented by Zhu [4–6]. In his opinion, the chaotic motion of a nonlinear VIS under a harmonic excitation with some parameters in a special range may appear, when part of the energy at the excitation frequency is distributed over a wide frequency brand because of the continuous spectrum of chaos. Therefore, if the import energy of the simple harmonic excitation is definite, the intensity of line spectrum at the primary harmonic frequency of the nonlinear VIS in chaotic state is definitely lower than that

*Corresponding author. Tel.: +86 27 83443241; fax: +86 27 83443990.
E-mail address: yuxiang_nue@sina.com (X. Yu).

0022-460X/$ - see front matter © 2007 Elsevier Ltd. All rights reserved.
doi:10.1016/j.jsv.2007.06.034

in nonchaotic state. Lou [6] confirmed the validity of this method through theoretical analyses and experiments. However, the parameters and operating mode of the nonlinear VIS may change in some conditions. If the parameters escape from the chaos parameter region, the motion of the nonlinear VIS will return to a periodic one, and the chaos method will lose its efficacy. Therefore, making the nonlinear VIS chaotic persistently, or preserving chaos of a chaotic nonlinear VIS, is meaningful and worth investigation for application of chaos to line spectra reduction, which also is the motivation of this paper. The aim of this paper is to develop a new method for maintaining chaos in the nonlinear VIS borrowing the principles of generalized synchronization (GS) of chaos.

Since the seminal work of Pecora and Carroll [7] on the synchronization of chaotic systems, synchronization phenomenon has formed a new body of research activities and various synchronization schemes, such as adaptive control [8], backstepping design [9], active control [10,11] and nonlinear control [12,13], have been successfully applied to chaos synchronization. However, most of the methods mentioned above synchronize two identical chaotic systems. In fact, for many practical systems such as laser array and biological system, it is impossible to assume that every component is identical. As a result, the synchronization of chaos between two different systems, which is known as GS of chaos, has drawn increasing attention in recent years. Yang [14] classified GS into three types: passive GS, resonant GS and interacting GS. In different types of GS, driving signal and response dynamics play different roles. Other works [15–17] focused on developing new control schemes for synchronizing different chaotic systems.

In this paper, the chaos method for reducing line spectra of the radiated noise of marine vessels is improved to become more realizable with the application of a driving parameter scheme to implement the chaotification of the nonlinear VIS. The scheme is similar to GS to a considerable degree since the nonlinear VIS as the response system is driven by an external chaotic system, which plays the role of drive system. The only difference between them is that the motion of the response system should exhibit chaos before being driven in GS but must be periodic in our scheme. Fortunately, the methods for analyzing the stability of GS are also suitable for our scheme, and hence we will explain the new method borrowing some principles and terms of GS. The rest of the paper is organized as follows. Section 2 describes the equations of motion of the nonlinear VIS and comments on the dynamic behavior of the coupled system. The definition and stability conditions of GS, as well as the driving parameter scheme, are studied in Section 3. Numerical simulations are carried out for confirming the validity and stability of this method in Section 4.

2. Equations of motion

It is necessary to consider the flexibility of the base for the VIS of onboard machinery. For simplification, the studied vibration will be confined to the low-frequency band. Under this condition, the flexible base can be reduced to a lumped mass and the whole nonlinear VIS can be considered as a two-degree-of-freedom (dof) mass–spring system. As shown in Fig. 1, M_1 and M_2 denote the isolated equipment and the base, respectively. M_1 is supported by a vibration isolator combining a liner damper and a nonlinear spring which possesses cubic nonlinearity. M_2 is connected with a fixed plane using a linear damper and a linear spring which is much harder than the nonlinear spring.

When the origins of coordinates are set at the places where the springs are not compressed, as shown in Fig. 1(a), the equations of the two-dof nonlinear spring–mass system can be formulated as follows:

$$\begin{aligned} &M_1\ddot{X}_1 + C_1(\dot{X}_1 - \dot{X}_2) + K_1(X_1 - X_2) + U_1(X_1 - X_2)^3 = F\cos\Omega t - M_1 g,\\ &M_2\ddot{X}_2 + C_2\dot{X}_2 + K_2X_2 = C_1(\dot{X}_1 - \dot{X}_2) + K_1(X_1 - X_2) + U_1(X_1 - X_2)^3 - M_2 g, \end{aligned} \tag{1}$$

where M_1 is the mass of the isolated equipment; M_2 is the mass of the base; C_1 is the damping coefficient of the nonlinear vibration isolator; K_1 and U_1 are the liner and cubic stiffness coefficients of the nonlinear vibration isolator, respectively; C_2 is the damping coefficient of the damper between the base and the fixed plane; K_2 is the stiffness coefficient of the liner spring between the base and the fixed plane; F and Ω are the amplitude and frequency of the harmonic excitation, respectively.

Note that the origins are not the equilibrium points of this system, which is inconvenient in further analyses, and so the coordinate transformation should be carried out. As shown in Fig. 1(b), the origins of the new

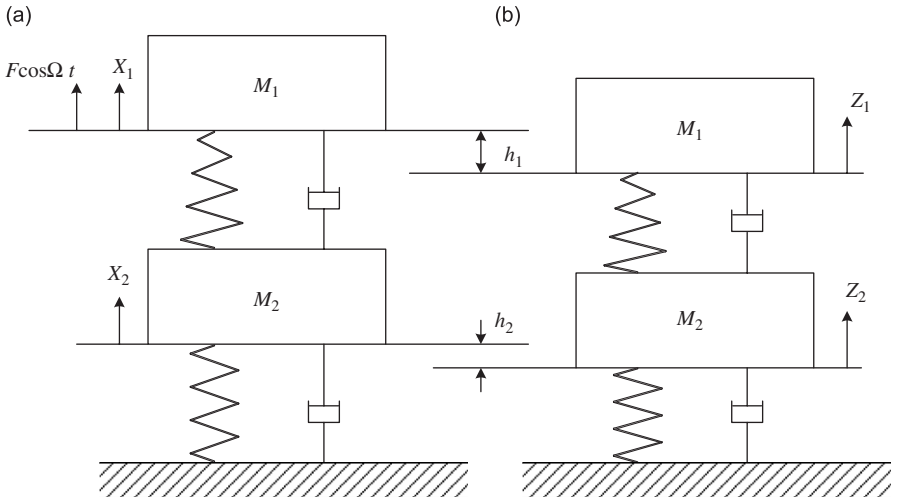

Fig. 1. Schematic diagram of the nonlinear VIS with two-degree-of-freedom.

coordinates are located at the equilibrium places of these springs, i.e. the places where these springs are compressed, and the relations between the old and new coordinates are:

$$X_1 = Z_1 - h_1, \quad X_2 = Z_2 - h_2. \tag{2}$$

When the system is in the equilibrium state, the following relations can be used to eliminate the gravitation terms from the right-hand side of the equations of motion:

$$\begin{aligned} K_1 H + U_1 H^3 &= M_1 g, \\ K_2 h_2 &= M_2 g + M_1 g, \end{aligned} \tag{3}$$

where $H = h_1 – h_2$. Substituting Eqs. (2) and (3) into Eq. (1), and using

$$\Omega_0 = \sqrt{\frac{M_1}{K_1 + 3U_1H^2}}, \quad Z_1 = Bx_1, \quad Z_2 = Bx_2, \quad B = \sqrt{\frac{K_1 + 3U_1H^2}{U_1}}, \quad T = \Omega_0 t,$$

the equations of motion under the new coordinates can be written in dimensionless and first-order form:

$$\begin{aligned} \dot{x}_1 &= y_1, \\ \dot{y}_1 &= -\delta_1(y_1 - y_2) - k_1(x_1 - x_2) + \xi_1(x_1 - x_2)^2 - (x_1 - x_2)^3 + f\cos\omega_1 t, \\ \dot{x}_2 &= y_2, \\ \dot{y}_2 &= -\mu\delta_2 y_2 - \mu k_2 x_2 + \mu\delta_1(y_1 - y_2) + \mu(x_1 - x_2) - \mu\xi_1(x_1 - x_2)^2 + \mu(x_1 - x_2)^3, \end{aligned} \tag{4}$$

where $\delta_1 = C_1 \Big/ \sqrt{M_1(K_1 + 3U_1H^2)}$, $\xi_1 = 3H/B$, $f = F/B(K_1 + 3U_1H^2)$, $\omega_1 = \Omega_0\Omega$, $\mu = M_1/M_2$, $\delta_2 = C_2 \Big/ \sqrt{M_1(K_1 + 3U_1H^2)}$, $k_1 = 1$, $k_2 = K_2/(K_1 + 3U_1H^2)$.

System (4) is a coupled oscillator with quadratic and cubic nonlinear terms. From the perspective of mathematics, the associated autonomous system possesses three equilibrium points: $A(0,0,0,0)$, $B(\frac{1}{2}\xi_1 + \frac{1}{2}\sqrt{\xi_1^2 - 4}, 0, 0, 0)$, $C(\frac{1}{2}\xi_1 - \frac{1}{2}\sqrt{\xi_1^2 - 4}, 0, 0, 0)$. However, for a practical nonlinear VIS, B and C are impossible because the relation between load and displacement is a monotone function and the curve of stiffness of the nonlinear spring has no chance to intersect the displacement axis more than two times. The free vibration of nonlinear VIS in some initial conditions will attenuate to the only equilibrium point A. Dynamics of this nonlinear VIS under a harmonic excitation is considerably complex. The typical nonlinear phenomena, such as attractor coexistence, jumping, bifurcation and chaos, can be observed in certain conditions. The literature is abundant with studies on this kind of coupled oscillator system. Kozlowski et al. [18] studied two

identical coupled double-well Duffing oscillators subjected to periodically driven force. Kenfack [19] investigated two-coupled double-well Duffing oscillators and discovered that period doubling of both types, symmetry breaking, sudden chaos and a great abundance of Hopf bifurcations exist in his model. Musielak et al. [20] studied chaos and routes to chaos in coupled Duffing oscillators with two-, four- and six-dof.

In our study, system (4) as the response system is driven by an additional chaotic system to make the chaotic motion persistent, and then the line spectra of radiated noise will be expected to be reduced. In the next section, we will present the driving parameter control scheme and discuss the stability conditions of this scheme.

3. Stability conditions and control scheme

3.1. Definition and stability conditions of GS

As mentioned above, some principles of GS will be adopted to develop a new control scheme to generate or maintain the chaotic motion in nonlinear VIS, and hence, the definition and stability conditions of GS are discussed first.

There are two types of couple modes in synchronization systems: bidirectional couple and unidirectional couple. The bidirectional couple mode means that the drive system and the response system affect each other, and in the unidirectional couple mode, only the response system may be acted by the drive system and the counteraction never happens. The method presented here is of the unidirectional couple mode.

Consider the unidirectional coupled systems of the following general form:

$$\dot{\mathbf{X}} = \mathbf{F}(\mathbf{X}), \tag{5a}$$

$$\dot{\mathbf{Y}} = \mathbf{G}(\mathbf{Y}) + k\mathbf{P}(\mathbf{X}, \mathbf{Y}), \tag{5b}$$

Here $\mathbf{X} = \{x_1, x_2, \ldots, x_d\}$ and $\mathbf{Y} = \{y_1, y_2, \ldots, y_r\}$ denote state vectors in d-dimensional space R^d and r-dimensional space R^r, respectively. $\mathbf{F}$ and $\mathbf{G}$ define the vector fields of the drive and response systems, respectively. **F:** $R^d \to R^d$, **G:** $R^r \to R^r$. $\mathbf{P}$ denotes a coupling term, and k is a scale factor defining the coupling strength.

Definition. When $k \neq 0$, the chaotic trajectories of the two systems are said to be synchronized in a generalized sense if there exists a transformation $\mathbf{\Phi}$: $\mathbf{X} \to \mathbf{Y}$ which is able to map asymptotically the trajectories of the drive attractor into the ones of the response attractor $\mathbf{Y} = \mathbf{\Phi}(\mathbf{X})$, regardless of the initial conditions in the basin of the synchronization manifold $M = \{(\mathbf{X}, \mathbf{Y}): \mathbf{Y} = \mathbf{\Phi}(\mathbf{X})\}$. The generalized synchronization of chaos will degenerate to the complete one if $\mathbf{\Phi}$ is an identical transformation.

The traditional method for analyzing the stability of differential equations is the Lyapunov function method. However, construction of an appropriate Lyapunov function is a difficult task for most of systems. Therefore, a method calculating the conditional Lyapunov exponents (CLEs) is adopted to analyze the stability of synchronizations.

Suppose the transformation $\mathbf{Y} = \mathbf{\Phi}(\mathbf{X})$ between the trajectories of the drive and response systems has been achieved. To determine the stability of the synchronization manifold $M = \{(\mathbf{X}, \mathbf{Y}): \mathbf{Y} = \mathbf{\Phi}(\mathbf{X})\}$, we add tiny perturbations $\mathbf{r}$ onto the driven trajectory $\mathbf{Y}$ and obtain $\mathbf{Y}' = \mathbf{\Phi}(\mathbf{X}) + \mathbf{r}$. Substituting $\mathbf{Y} = \mathbf{\Phi}(\mathbf{X})$ into Eq. (5b), the response system can be rewritten as

$$\dot{\mathbf{\Phi}}(\mathbf{X}) = \mathbf{G}(\mathbf{\Phi}(\mathbf{X})) + k\mathbf{P}(\mathbf{X}, \mathbf{\Phi}(\mathbf{X})). \tag{6}$$

Substituting $\mathbf{Y}' = \mathbf{H}(\mathbf{X}) + \mathbf{r}$ into Eq. (5b) and considering Eq. (6), we obtain

$$\dot{\mathbf{r}} = \mathbf{G}(\mathbf{\Phi}(\mathbf{X}) + \mathbf{r}) + k\mathbf{P}(\mathbf{X}, \mathbf{\Phi}(\mathbf{X}) + \mathbf{r}) - \mathbf{G}(\mathbf{\Phi}(\mathbf{X})) - k\mathbf{P}(\mathbf{X}, \mathbf{\Phi}(\mathbf{X})). \tag{7}$$

Using Taylor expansions and omitting the high-order terms, Eq. (7) can be changed into

$$\dot{\mathbf{r}} = (\mathbf{D}_{\mathbf{\Phi}}\mathbf{G}(\mathbf{\Phi}(\mathbf{X})) + k\mathbf{D}_{\mathbf{\Phi}}\mathbf{P}(\mathbf{X}, \mathbf{\Phi}(\mathbf{X})))\mathbf{r}, \tag{8}$$

where $(\mathbf{D}_{\mathbf{\Phi}}\mathbf{G}(\mathbf{\Phi}(\mathbf{X})) + k\mathbf{D}_{\mathbf{\Phi}}\mathbf{P}(\mathbf{X},\mathbf{\Phi}(\mathbf{X})))$ is the Jacobian matrix and let it be $\mathbf{A}(\mathbf{X})$. According to the first-order approximation theorem, if all the eigenvalues of the Jacobian matrix possess negative real parts, the zero solution of the perturbed equation (8) is asymptotically stable, i.e., the synchronization manifold $M = \{(\mathbf{X}; \mathbf{Y}): \mathbf{Y} = \mathbf{\Phi}(\mathbf{X})\}$ is stable. However, it should be noted that the driving signal $\mathbf{X}$ in Jacobian matrix $\mathbf{A}(\mathbf{X})$ is governed by the map $\mathbf{X} = \varphi(\mathbf{X}_0, t)$, where φ is the solution of the drive system, $\mathbf{X}_0$ is the initial condition and t is the time variable. In this situation, the Jacobian matrix $\mathbf{A}(\mathbf{X})$ can be expressed as $\mathbf{A}(t)$ and its eigenvalues also change with time, and hence the stability of the zero solution of the perturbed equation (8) should be determined by the time-varying characteristics of the eigenvalues of the matrix $\mathbf{A}(t)$ instead of the eigenvalues at a fixed time point. Lyapunov exponents (LEs) just play this role in the description of the evolutional behavior with time of dynamical systems. They measure the average rate of divergence or convergence of trajectories starting from nearby initial points. Therefore, they can be used to analyze the stability of limits sets and to check sensitive dependence on initial conditions, and can be calculated numerically from the perturbed equation with some standard schemes. The LEs are said to be conditional if the Jacobian matrix of the perturbed equation not only includes the variables of itself but also depends on the outputs of other system. So the CLEs are often used to analyze the stability of synchronization of chaos and some chaotification schemes.

The CLEs can be obtained from Eq. (8) with numerical calculations, which is similar to the calculations of LEs, and the maximum CLE is expressed as

$$\lambda_{max} = \lim_{t\to\infty} \frac{1}{t} \ln\left(\frac{||\mathbf{r}(t)||}{||\mathbf{r}(0)||}\right). \tag{9}$$

Consequently, the necessary condition of asymptotic stability of the system (5b) is $\lambda_{\max} < 0$ (this is also a sufficient condition for most situations).

3.2. Control scheme

At present, increasing number of researchers realize that sometimes chaotic behavior and chaos synchronization are beneficial and desirable in many applications. For this purpose, making a non-chaotic dynamical system chaotic or retaining (or enhancing) the chaos of a chaotic system is called ''anti-control of chaos'' or ''chaotification''. The primary chaotification schemes for a nonlinear dynamical system include feedback control [21–23], adaptive control [24,25], switching piecewise-linear control [26,27], and so on. Among these methods, the feedback control is the most popular method for its simple configuration and easy implementation.

For generating chaos in the nonlinear VIS of onboard machinery, the feedback scheme means that the execute components should be connected with the isolated equipment or the base directly, and hence have to consume considerable energy and occupy larger space for achieving the designed control aim. However, the energy and space in marine vessels are limited strictly, and this impels us to develop a new control scheme with a little energy consumption as well as an excellent control performance. In this paper, the driving parameter scheme as an appropriate method is presented.

In the driving parameter scheme, some parameters of the nonlinear VIS such as the stiffness or damping coefficients are defined as a function of output of the driving chaotic system. In this way, the response of the nonlinear VIS will follow after the chaotic driving signal in a generalized sense and the persistent chaos in the response system, i.e. the nonlinear VIS, may be realized conveniently since the driving signal always preserves chaos. At the same time, energy consumption may be confined to an acceptable level because some parameters of the nonlinear VIS may change sharply with tiny input energy.

The driving chaotic system is selected as

$$\begin{aligned} \dot{u} &= v, \\ \dot{v} &= -u - u^3 - av + b\cos\omega t + G. \end{aligned} \tag{10}$$

This system is a typical single-dof oscillator excited by a harmonic force, and the difference from Duffing equation is gravitation term G appears on the right-hand side of the second equation. When $a = 0.1$, $b = 9$, $G = 2$, $\omega = 3.9311$, two attractors, one is chaotic and the other is period-1, coexist in the phase plane of this

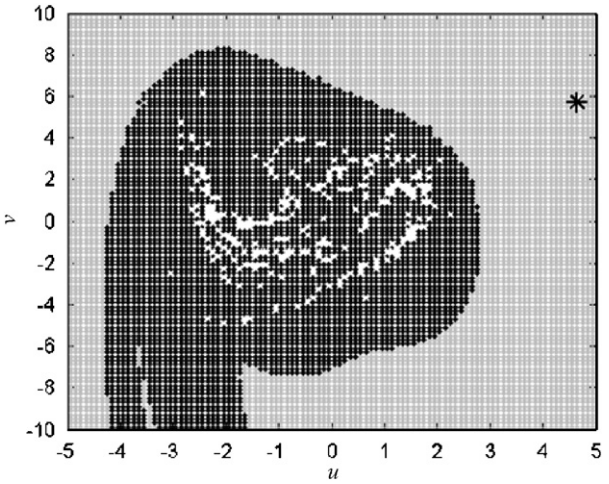

Fig. 2. Two coexistent attractors and their basins of the drive system. Symbol * and the gray area denote the period-1 attractor and its basin, respectively, and white dots and black area denote the chaotic attractor and its basin, respectively.

system. These attractors and their basins are shown in Fig. 2, from which we can select an appropriate initial point to ensure the drive system exhibits chaotic behavior. Without loss of generality, the initial condition is selected as (0, 0), and the phase portrait and Poincaré map of the chaotic motion are shown in Fig. 3. The driving chaotic system can be realized using a circuit system easily, and the circuit diagram is shown in Fig. 4.

System (4) as the driven system will be modified to a parameter-variable system according to the driving parameter scheme. The stiffness and damping coefficients can be selected as variable parameters, as they depend on the requirements in engineering. Consider now the dimensionless linear stiffness k_1 as a function of the output v of the drive system (10) in which we have proportional function, $k_1 = pv$, the simplest case, and then the response system can be rewritten as the following form:

$$\begin{aligned}
&\dot{x}_1 = y_1,\\
&\dot{y}_1 = -\delta_1(y_1 - y_2) - pv(x_1 - x_2) + \xi_1(x_1 - x_2)^2 - (x_1 - x_2)^3 + f\cos\omega_1 t,\\
&\dot{x}_2 = y_2,\\
&\dot{y}_2 = -\mu\delta_2 y_2 - \mu k_2 x_2 + \mu\delta_1(y_1 - y_2) + \mu(x_1 - x_2) - \mu\xi_1(x_1 - x_2)^2 + \mu(x_1 - x_2)^3,
\end{aligned} \tag{11}$$

where p is the driving factor. According to the definition of GS, it is obvious that the drive system (10) and response system (11) may be constructed as a GS system if the motion of the response system (11) is chaotic in the absence of drive. However, for the nonlinear VIS in engineering, the operating modes in most situations are the periodic motions, which is also the reason why chaos is hoped to be introduced into the nonlinear VIS to reduce the line spectra of the radiated noise. Therefore, the driving parameter scheme presented above does not satisfy the definition of GS exactly, but actually a type of synchronization, similar to GS, may be achieved between the driving signal and the response of the system (11) and the CLEs can also be used to analyze the stability of this scheme.

For the response system (11), the driving signal v can be regarded as the time-dependent perturbation added to the dimensionless line stiffness and plays a role similar to the external force $f\cos(\omega_1 t)$. When other parameters are fixed and the diving factor p is large enough, response of system (11) is expected to be a function of the driving signal v, which is the essential characteristic of the GS, and hence, we also consider this phenomenon as a type of synchronization, and the synchronization manifold is expressed as $M = \{(\mathbf{X}; \mathbf{Y}): \mathbf{Y} = \mathbf{\Phi}(\mathbf{X})\}$ ($\mathbf{X} = \{u, v\}$, $\mathbf{Y} = \{x_1, y_1, x_2, y_2\}$).

As discussed in Section 3.1, the CLEs are used to characterize the divergence or the convergence of the tangent space along with the trajectory of the response system, which is synchronized with the trajectory of the drive system. The negative maximum CLE means trajectories originating from the neighborhood of the synchronization manifold will be attracted into the synchronized trajectory, which is applicable not only for

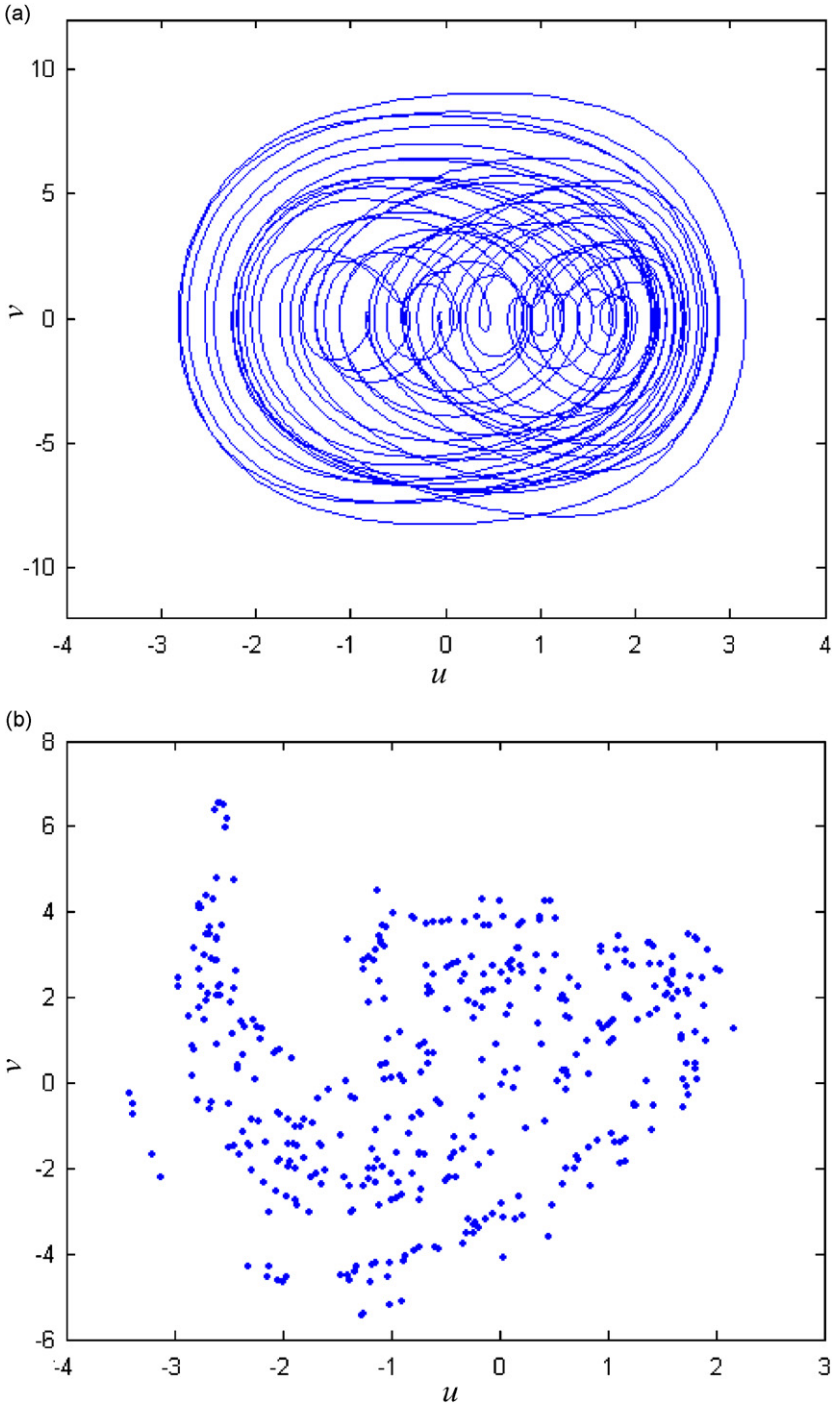

Fig. 3. Phase portrait (a) and Poincaré map (b) of the drive system.

the GS but also for the synchronization defined here. Therefore, the maximum CLE is used for analyzing the stability of the driving parameter schemes in numerical simulations.

Now the driving parameter method is summarized: select appropriate parameters to ensure the drive system (10) is chaotic and use the chaotic output v to drive the dimensionless line stiffness of response system (11) to realize persistent chaotic motion in the nonlinear VIS. In this way, the chaotic motion obtained in the

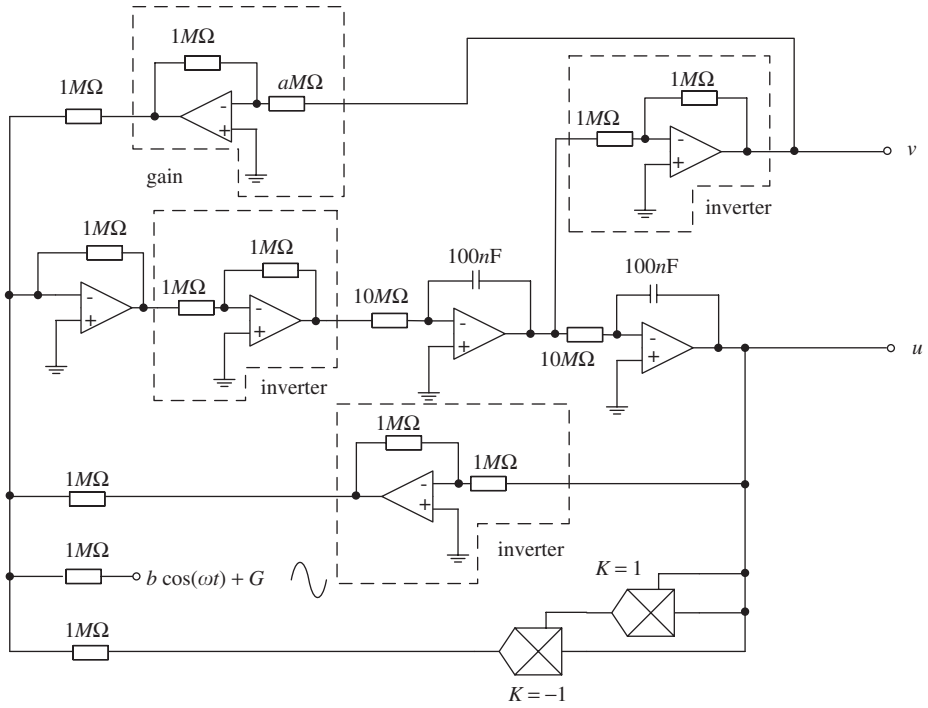

Fig. 4. Circuit diagram of the drive system.

nonlinear VIS leads to considerable reduction of line spectra of the radiated noise which will be confirmed through numerical simulations in Section 4.

4. Numerical simulations

The following numerical simulations demonstrate and verify the effectiveness and stability of the proposed driving parameter control scheme. The fourth-order Runge–Kutta method is used to integrate the differential equations with time step 0.01.

4.1. Effectiveness

Because vibration of onboard equipments is transmitted to the hull primarily through the base, comparison of vibration of the base between cases under drive and free from drive is carried out first.

In the absence of drive, nonlinear VIS takes on a periodic motion with $\delta_1 = \delta_2 = 0.2$, $\xi_1 = 1$, $f = 20$, $\mu = 0.2$, $k_2 = 2$, $\omega_1 = 3.9311$, and the phase portrait and power spectrum of the base are shown in Fig. 5. When the parameter of nonlinear VIS is driven by the external chaotic system with driving factor $p = 0.1$, the motion of the response system is typically chaotic, as shown in Fig. 6, which illustrates the phase portrait and power spectrum of the driven chaotic motion of the base. Comparing Fig. 5(b) with Fig. 6(b), it is obvious that the intensity of line spectra at the primary frequencies as well as the whole spectrum of the driven motion is much less than those of the periodic motion. In Fig. 5(b), the average of the whole spectrum of the base in the uncontrolled case is 3.92 dB and the line spectrum at the primary frequency $\omega_1 = 3.9311$ is 39.95 dB. The corresponding values of the driven chaotic motion are −17.51 and 15.64 dB, as shown in Fig. 6(b), and hence reductions are 21.43 and 24.31 dB respectively. The notable reduction of the whole spectrum between those two cases means the capability of vibration isolation of nonlinear VIS has been improved considerably when the driven chaotic motion is achieved. Furthermore, under this condition, the nonlinear VIS also possesses excellent performance for reducing and eliminating line spectra, which are bound to exist at periodic motions.

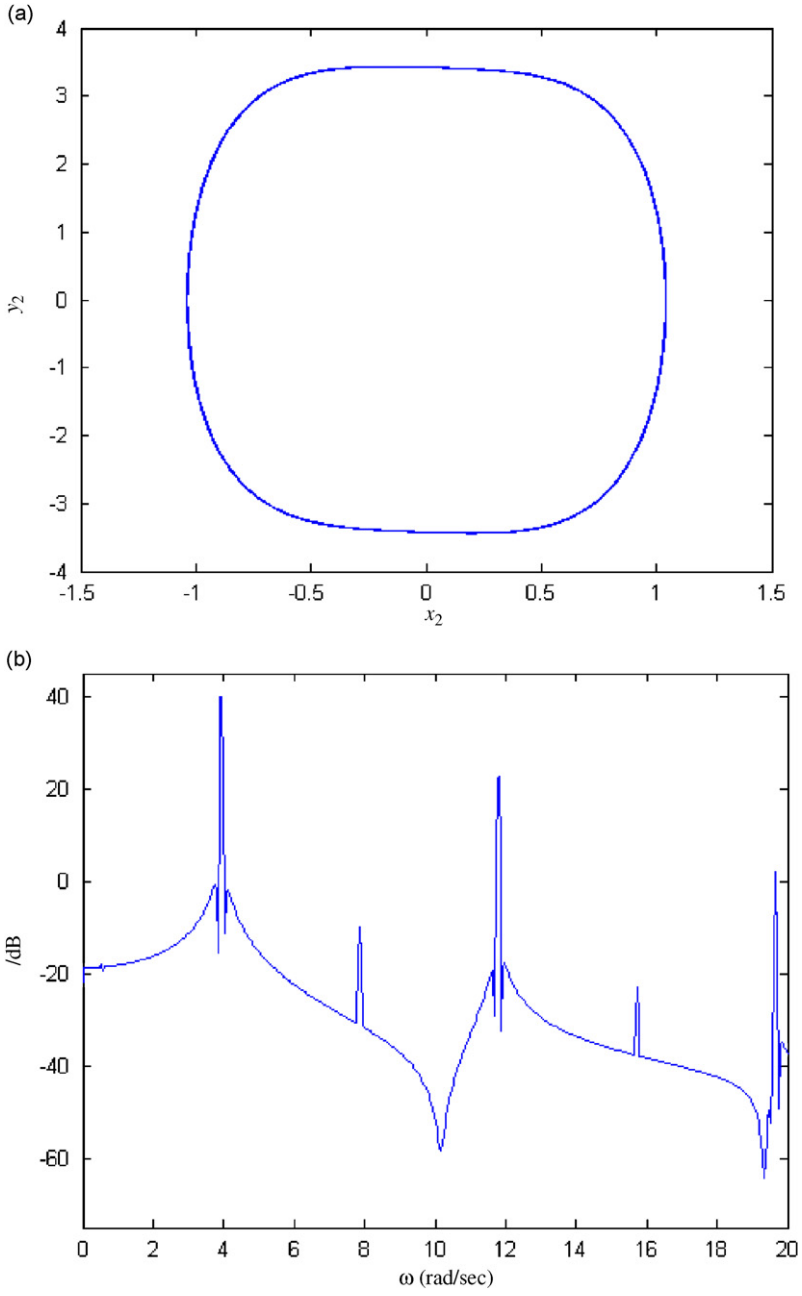

Fig. 5. Phase portrait (a) and power spectrum (b) of the base M_2 in the uncontrolled state.

Effectiveness of this method has been demonstrated as discussed above. However, there is still a question: Does the good performance in driven chaotic state result from decrease of line stiffness? As shown in Fig. 3, the maximum of driving signal v is approximately 9. So the driven parameter $k_1 = pv$ with $p = 0.1$ is slightly less than the original value 1. For traditional VIS, less stiffness always implies more vibration loss between the isolated equipment and the base, especially for low-frequency vibrations. However, as we know, decreasing the stiffness may result in instability of the VIS and enlargement of the vibration amplitude of the isolated equipment, as is the reason why the vibration level of the isolated equipment is as another important performance index. For the nonlinear VIS operated in the driven chaotic state, it will be confirmed that the

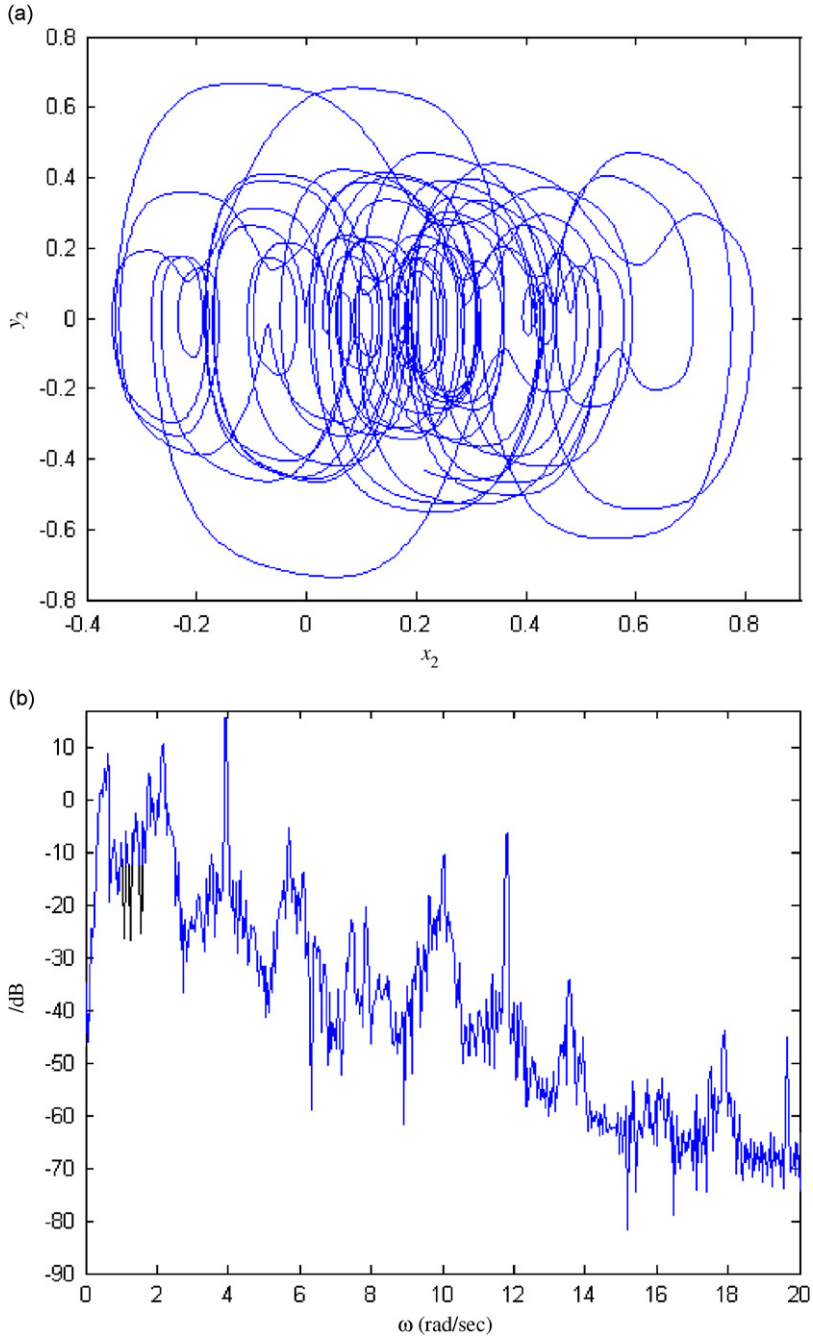

Fig. 6. Phase portrait (a) and power spectrum (b) of the base M_2 in the controlled state.

remarkable effectiveness is independent, at least partly, of the decrease of the stiffness because the vibration of the isolated equipment can also be suppressed when the driven chaotic motion is realized.

The time histories of displacements of the isolated equipment with driving signal and without it are shown in Fig. 7. The dashed line denotes the case free from being driven and the solid line denotes the driven one. From this figure, it is obvious that the amplitude of the isolated equipment is suppressed when the driving parameter method is applied, which is another advantage of this method and can be used to verify that the effectiveness

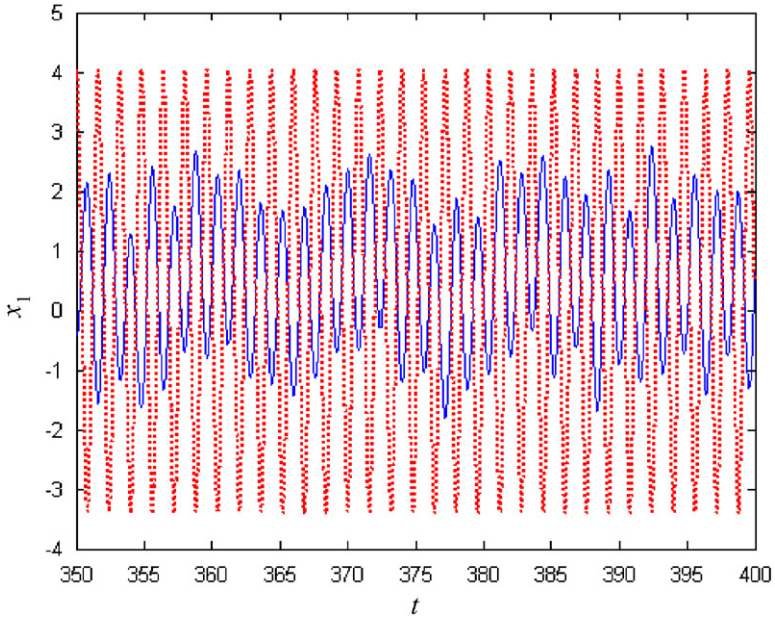

Fig. 7. Time histories of the displacements of isolated equipment M_1 in the uncontrolled state (dashed line ⋯) and controlled state (solid line —).

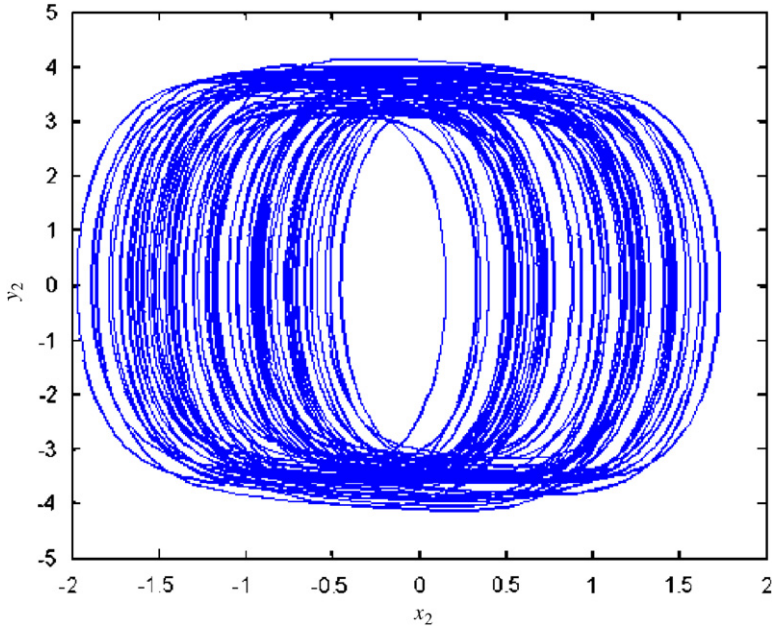

Fig. 8. Phase portrait of the base M_2 at $p = 0.21$.

of the nonlinear VIS in the controlled chaotic state has little connection with the decrease of the nonlinear stiffness.

As discussed above, one can find that the appropriate selection of the driving factor p is very important for this driving parameter scheme. On the one hand, vibration of the isolated equipment will not be suppressed or

even amplified if the driving factor p is too small and, on the other hand, with increasing p, the system bifurcate into another attractor at $p = 0.21$, which exhibits more violent behavior, as shown in Fig. 8. Therefore, only the moderate values can be selected as the driving factors for the purpose of reducing line spectra of the structure-borne noise, as well as suppressing the vibration of the isolated equipment.

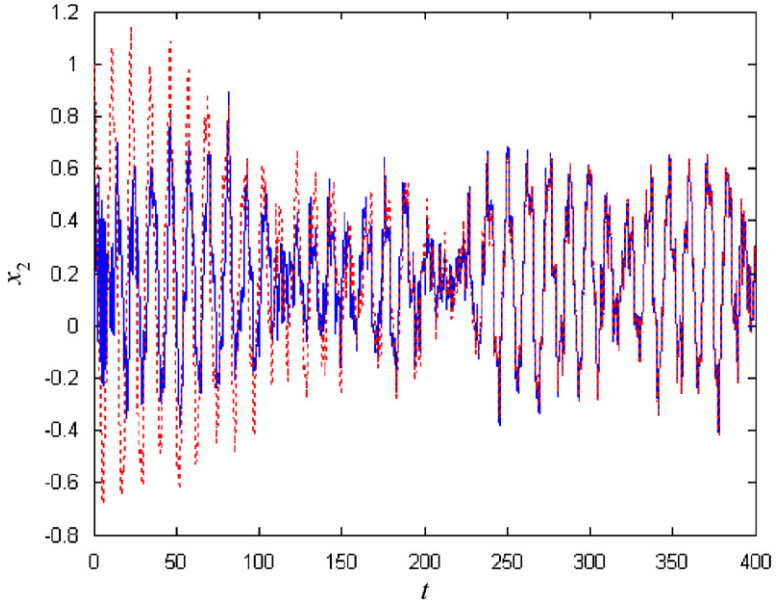

Fig. 9. Time histories of x_2 originating from different initial conditions. Solid line (—) denotes the case from the initial condition (0, 0, 0, 0), and dashed line (···) is from (0,0,1,0.1).

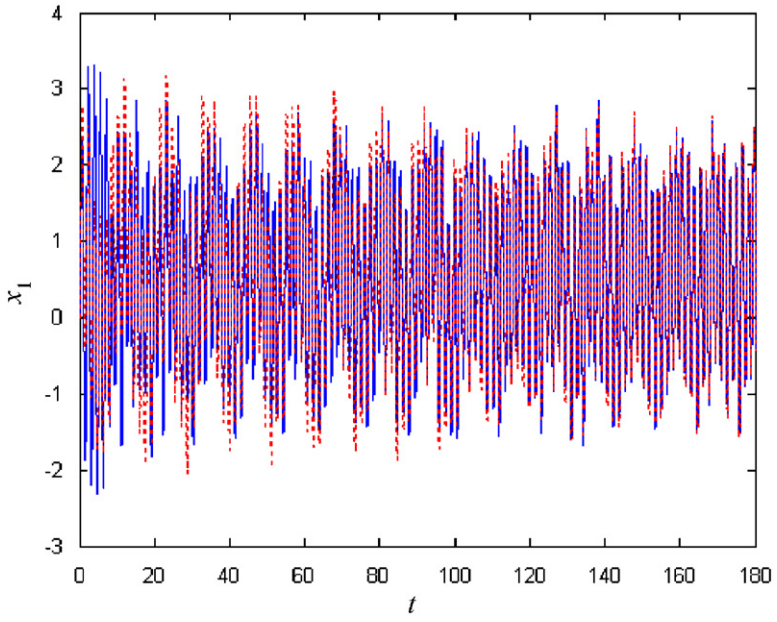

Fig. 10. Time histories of x_1 originating from different initial conditions. Solid line (—) denotes the case from the initial condition (0, 0, 0, 0), and dashed line (···) is from (0, 0, 1, 0.1).

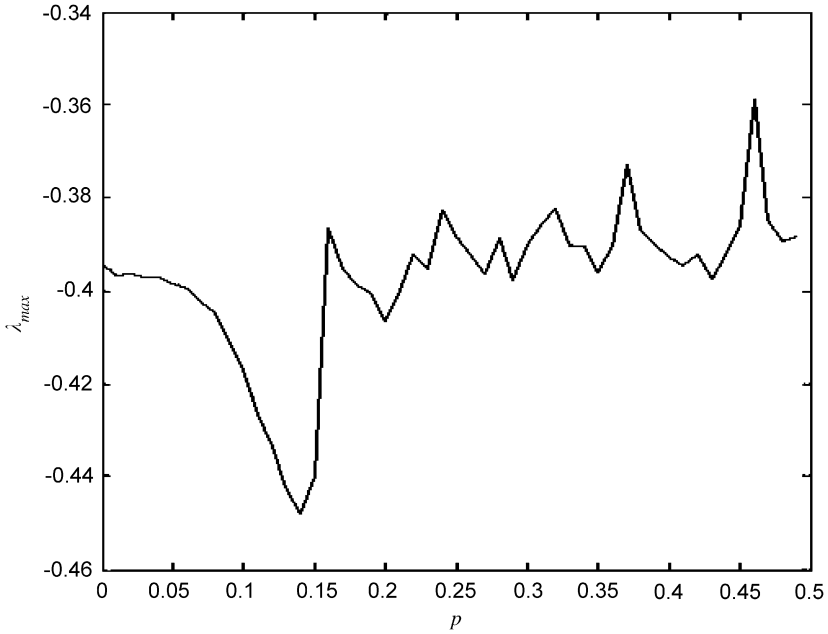

Fig. 11. Maximum CLE versus the driving factor p.

4.2. Stability

As mentioned above, stability of synchronization refers to asymptotic stability of the response system, i.e., the motion will trend to the same response attractor at arbitrarily different initial conditions in a neighborhood of the synchronization manifold when synchronization is realized. As shown in Fig. 9, solid line denotes the time history of the displacement x_2 of the base originating from the initial condition (0,0,0,0) and dashed line denotes the time history of x_2 from the initial condition (0,0,1,0.1). As shown in this figure, motions coincide with each other very soon after a short transient process. The same phenomena can be found in Fig. 10, which shows the counterparts of the isolated equipment.

Further consideration about the stability of the driving parameter scheme is to calculate the maximum CLE which as a practicable tool is usually used to analyze the stability of GS. Here, the maximum CLE of the system considered in this paper is calculated numerically and the results are shown in Fig. 11. This figure shows the variation of the maximum CLE versus the driving factor p. The CLE is negative at each p despite the existence of fluctuation. Therefore, the stability of the driving parameter scheme can be confirmed through above analyses.

5. Conclusions

Chaos can be used to reduce the linear spectra of the radiated noise of marine vessels because of its continuous spectrum. However, in practice, parameters of nonlinear VIS may change in some circumstances and, as a result, the motion is likely to return to a periodic one. How to obtain persistent chaos is the key step to realize the chaos method for reducing the line spectra of the radiated noise. In this paper, the driving parameter method using the external driving signal to drive the nonlinear VIS is presented to generate persistent chaos in the nonlinear system, and thus we use the chaos method for reducing the linear spectrum.

Numerical simulations are carried out to confirm the validity and stability of this method. The results show that utilizing this method nonlinear VIS not only possesses an excellent isolation performance of vibration and line spectra, but also reduce the amplitude of the isolated equipment notably. The energy required in this method is much smaller than that in other control schemes. The maximum CLEs are calculated at different driving factors p and the negative values demonstrate the stability of this method.

Acknowledgment

This work is supported by the National Natural Science Foundation of China (Grant no. 50675220).

References

[1] C.C. Wang, J.P. Su, A new adaptive structure control for chaotic synchronization and secure communication, *Chaos, Solitons & Fractals* 20 (2004) 967–977.
[2] M. Lakshmanan, K. Murali, *Chaos in Nonlinear Oscillators: Controlling and Synchronization*, World Scientific, Singapore, 1996.
[3] B. Blasius, A. Huppert, L. Stone, Complex dynamics and phase synchronization in spatially extended ecological systems, *Nature* 399 (1999) 354–359.
[4] S.J. Zhu, Chaotic technique research for noise-reduction and vibration-isolation systems on warships, PhD Thesis, National University of Defense Technology, China, 2006 (in Chinese).
[5] R.J. Jiang, S.J. Zhu, L. He, Prospect of applying controlling chaotic vibration in waterborne-noise confrontation, *Proceeding of ASME 2001 Design Engineering Technical Conference and Computers and Information in Engineering Conference*, Pittsburgh, September, 2001, DETC 2001/VIB-21663.
[6] J.J. Lou, S.J. Zhu, L. He, X. Yu, Application of chaos method to line spectra reduction, *Journal of Sound and Vibration* 286 (2005) 645–652.
[7] L.M. Pecora, T.L. Carroll, Synchronization of chaotic systems, *Physical Review Letters* 64 (1990) 821–824.
[8] S.H. Chen, J. Lü, Synchronization of an uncertain unified system via adaptive control, *Chaos, Solitons & Fractals* 14 (2002) 643–647.
[9] X. Tan, J. Zhang, Y. Yang, Synchronizing chaotic systems using backstepping design, *Chaos, Solitons & Fractals* 16 (2003) 37–45.
[10] Y.M. Lei, W. Xu, H.C. Zheng, Synchronization of two chaotic nonlinear gyros using active control, *Physics Letters A* 343 (2005) 153–158.
[11] Y.M. Lei, W. Xu, J.W. Shen, T. Fang, Global synchronization of two parametrically excited systems using active control, *Chaos, Solitons & Fractals* 28 (2006) 428–436.
[12] L. Huang, R. Feng, M. Wang, Synchronization of chaotic systems via nonlinear control, *Physics Letter A* 320 (2004) 271–275.
[13] H.K. Chen, Global chaos synchronization of new chaotic systems via nonlinear control, *Chaos, Solitons & Fractals* 23 (2005) 1245–1251.
[14] J. Yang, G. Hu, Three types of generalized synchronization, *Physics Letters A* 361 (2007) 332–335.
[15] H.K. Chen, Synchronization of two different chaotic systems: a new system and each of the dynamical systems Lorenz, Chen and Lu, *Chaos, Solitons & Fractals* 25 (2005) 1049–1056.
[16] R.M. Allister, A. Uchida, R. Meucci, R. Roy, Generalized synchronization of chaos: experiments on a two-mode microchip laser with optoelectronic feedback, *Physica D* 195 (2004) 244–262.
[17] R. Femat, J.A. Ramirez, Synchronization of a class of strictly different chaotic oscillators, *Physics Letters A* 236 (1997) 307–313.
[18] J. Kozlowski, U. Parlitz, W. Lauterborn, Bifurcation analysis of two coupled periodically driven Duffing oscillators, *Physical Review E* 51 (1995) 1861–1867.
[19] A. Kenfack, Bifurcation structure of two coupled periodically driven double-well Duffing oscillators, *Chaos, Solitons & Fractals* 15 (2003) 205–208.
[20] D.E. Musielak, Z.E. Musielak, J.W. Benner, Chaos and routes to chaos in coupled Duffing oscillators with multiple degrees of freedom, *Chaos, Solitions & Fractals* 24 (2005) 907–922.
[21] Z. Wang, K.T. Chau, Anti-control of chaos of a permanent magnet DC motor system for vibratory compactors. *Chaos, Solitons & Fractals* doi:10.1016/j.chaos.2006.06.105 (unpublished).
[22] H.K. Chen, C.I. Lee, Anti-control of chaos in rigid body motion, *Chaos, Solitons & Fractals* 21 (2004) 957–965.
[23] P. Saha, S. Banerjee, A.R. Chowdhury, On the study of control and anti-control in magnetoconvection, *Physics Letters A* 306 (2003) 211–226.
[24] H.G. Zhang, Z.L. Wang, D.R. Liu, Chaotifying fuzzy hyperbolic model using adaptive inverse optimal control approach, *International Journal of Bifurcation and Chaos* 14 (2004) 3505–3517.
[25] Z.M. Ge, C.I. Lee, Control, anticontrol and synchronization of chaos for an autonomous rotational machine system with time-delay, *Chaos, Solitons & Fractals* 23 (2005) 1855–1864.
[26] J. Lü, G. Chen, A new chaotic attractor coined, *International Journal of Bifurcation and Chaos* 12 (2002) 659–661.
[27] Z.H. Zheng, J.H. L ü, G.R. Chen, T.S. Zhou, S.C. Zhang, Generating two simultaneously chaotic attractors with a switching piecewise-linear controller, *Chaos, Solitons & Fractals* 20 (2004) 277–288.